Post-CCA and Reinforcement Learning Based Bandwidth Adaptation in 802.11ac Networks

Seowoo Jang, *Student Member, IEEE*, Kang G. Shin, *Life Fellow, IEEE*,
and Saewoong Bahk, *Senior Member, IEEE*

Abstract—The new 802.11ac standard aims at achieving Gbps data throughput for individual users by exploiting enhanced physical-layer features, such as higher modulation levels, Multiple Input Multiple Output (MIMO), and wider bandwidths. However, the heterogeneity of bandwidth in a network can cause asymmetric interferences in which certain transmissions cannot be sensed by some other nodes. As a result, the conventional Carrier Sense Multiple Access with Collision Avoidance (CSMA/CA) may not work well in 802.11ac networks. We call this the *Hidden Channel* (HC) problem, which is shown to be *real* via experiments with USRP and WARP boards. To solve this problem, we propose bandwidth adaptation based on *post-CCA*, which is a clear channel assessment (CCA) procedure performed *after* completing a transmission. Post-CCA in wireless networks helps mimic the CSMA with Collision Detection (CSMA/CD) mechanism in the wired Ethernet, thus enhancing channel assessment capability. Using post-CCA, we propose Post-CCA based Bandwidth Adaptation (PoBA) that alters bandwidth and channel configuration dynamically by applying a reinforcement learning mechanism. Post-CCA and PoBA do not require any hardware modification and are also compliant with the 802.11 standards. PoBA is shown via simulation to increase network-wide throughput, channel utilization and fairness, and also lower packet error probability.

Index Terms—Hidden channel problem, post-CCA, bandwidth adaptation, 802.11ac, reinforcement learning, POMDP

---

1 INTRODUCTION

OVER the last decade, we have witnessed a dramatic increase in mobile data traffic due to the large-scale deployment of increasingly powerful mobile devices and the resulting proliferation of mobile services/applications. This trend is expected to continue in the foreseeable future [5]. To deal with this explosive growth of mobile traffic, there have been numerous efforts to increase wireless link/network capacity by developing new physical-layer technologies and/or improving the existing design. However, these solutions are still unable to keep up with fast growing demands.

Bandwidth has been allocated and used statically until recently. For example, 802.11a/b/g uses one of 11 predefined channels, each with 20 MHz bandwidth in 2.4 GHz band. Also, even though 3GPP Long Term Evolution (LTE) allows 1.25-20 MHz, a system is required to choose one of the allowed bandwidths and a corresponding channel. However, the advances of hardware technology have made it possible to use wider bandwidths as defined in 802.11n and 802.11ac [9], [10] or dynamically change bandwidth according to the surrounding environments of a link as in [13], [14], [15], [16].

The wider and dynamically changing bandwidth introduces heterogeneous bandwidths to local area networks. 802.11n networks with up to 40 MHz bandwidth will likely coexist with 802.11ac with up to 160 MHz bandwidth in 5 GHz band. Furthermore, cellular systems also enhance wireless capacity with bandwidth-related approaches [22], [23]. For example, LTE-U (LTE in Unlicensed band), LAA-LTE (Licensed Assisted Access-LTE) and LWA (LTE WiFi Link-Aggregation) [6], [7] are planning to make use of unlicensed spectrum at 5 GHz band along with its cellular band. Thus, next-generation local area networks need to manage and handle problems caused by heterogeneous bandwidths to offer better user experiences.

Recently, the 802.11 Working Group initiated the development of the next version, 802.11ax [8], [21], including not just enhancement of the physical-layer but also medium-access and network-layer technologies. The next-generation Wireless Local Area Networks (WLANs) will be deployed in an environment where a large number of access points (APs) coexist to achieve higher throughput. In such an environment, it is important to resolve medium-access and network-layer conflicts. So, the 802.11 standardization committee has been working on the problems related to the MAC and the network layer to make them operate more efficiently.

To deal with heterogeneous bandwidth systems, 802.11ac has a mechanism to incorporate the extended, heterogeneous bandwidths (20/40/80/160/80+80 MHz) into channel assessment and contention, and to provide backward compatibility with the legacy versions using only 20 MHz bandwidth. The mechanism is a modification of the conventional Listen-before-Talk, or Carrier Sense Multiple Access with Collision Avoidance (CSMA/CA). Clear Channel Assessment (CCA) is performed on a 20 MHz channel or on the primary/secondary

---

- *S. Jang and S. Bahk are with the School of Electrical Engineering, INMC, Seoul National University, Gwanak-gu, Seoul 151-742, Korea. E-mail: {swjang, sbahk}@netlab.snu.ac.kr.*
- *K.G. Shin is with the Department of Electrical Engineering and Computer Science, University of Michigan, Ann Arbor, MI 48109. E-mail: kgshin@umich.edu.*

channel separately. Due to the hardware complexity and network design philosophy, the CCA sensitivities used for both types of channel are different [9], [11], [17], [18].

Also, due to the limited maximum transmit power at a transmitter regardless of the bandwidth used, the CCA capability on each channel or of each transceiver can vary. If the difference is large enough, then two transmission-attempting devices will have different channel assessments. This results in one-way interference just like the hidden terminal problem. The problem should be resolved because the one-way interference always makes some transmissions experience interruptions, causing a very high packet error rate.

For simplicity, we use 802.11ac as a reference system in this paper, and show that the conventional CSMA/CA may not work well due to the hidden channel (HC) problem in emerging local area communication networks with heterogeneous bandwidths. The HC problem [11], [17], [18] is similar to the well-known hidden terminal problem, which is caused by the discordance between the physical locations of a transmitter assessing channel idleness and a receiver experiencing actual conflicts. The CCA result at the transmitter is correct but a collision can happen. The RTS-CTS handshaking has been proposed to resolve the disharmony of spatial reservation by sending small control packets from both sender and receiver sides. In contrast to the hidden terminal problem, the HC problem arises from the discrepancy of bandwidth usage. In other words, the hidden channel problem makes the CCA result unreliable. Since RTS/CTS control messages themselves can also suffer the HC problem, the RTS-CTS handshaking cannot completely solve it, thus calling for a new solution to the spectral reservation discrepancy.

This paper makes the following key contributions.

- Confirmation of the HC problem in real 802.11ac networks. Specifically, we conducted simple experiments with WARP v.3 [1] and USRP [2], and showed the existence of the HC problem in real WLANs. Then the severeness of the HC problem in a network scenario and the effect of the CCA sensitivity gap have been presented.
- Proposal of a simple yet effective operation called '*post-CCA*' that senses channel idleness again after completing a transmission. Post-CCA is standard-compliant, and can be applied without hardware modification.
- Development of a novel solution, called the *PoBA* (Post-CCA based Bandwidth Adaptation), to the HC problem that dynamically changes bandwidth and channel configuration to avoid the one-way interference by using the post-CCA operation in a distributed manner. PoBA is modeled with Partially Observable Markov Decision Process (POMDP) by exploiting that the HC problem has partial observability. Like post-CCA, PoBA is also standard-compliant. To the best of our knowledge, this is the first to propose post-CCA operation in WLANs and the corresponding learning based bandwidth-channel adaptation.
- Detailed evaluation of the performance of PoBA. PoBA reduces the packet error rate by 5 percent and increases the throughput by 10 to 30 percent, on average, over the standard scheme in dense networks.
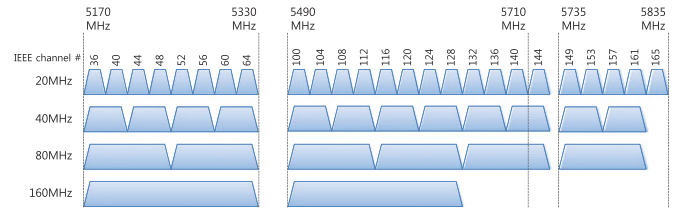

Fig. 1. Channelization of 802.11ac in the USA.

The rest of this paper is organized as follows. The contention mechanism for incorporating extended bandwidths in 802.11ac and the effect of bandwidth selection are presented in Section 2 as prerequisites. Then, the asymmetric interference (i.e., HC) problem is illustrated in Section 3. By conducting simple experiments, we also show that the HC problem is real. The ideas of post-CCA and PoBA algorithms are detailed in Sections 4 and 5. Using simulation, PoBA is shown in Section 6 to significantly enhance the network performance. The related work is discussed in Section 7 and finally, the paper is concluded in Section 8.

2 BACKGROUND

2.1 802.11ac Extended Bandwidth

A major goal of IEEE 802.11ac is to offer a very high throughput (VHT) while guaranteeing backward compatibility. Of many new features to achieve this goal, *extended bandwidth* is unique and distinct from the previous versions. 802.11ac allows to use only non-overlapping channels, as illustrated in Fig. 1 [9], [17], [18], [19]. Two adjacent 20 MHz channels can be merged/bonded as a 40 MHz channel, and two adjacent 40 MHz channels as an 80 MHz channel. A 160 MHz channel can be formed either by merging two adjacent or non-adjacent 80 MHz channels. This feature is inherited from the design concept of 802.11n [10] to avoid in-band interference within the maximum bandwidth of 40 MHz.

For the purpose of contention resolution, 802.11ac defines *primary* and *secondary* channels. A station chooses a 20 MHz as a primary channel to guarantee backward compatibility with legacy stations working only on a 20 MHz channel, and compatibility among 802.11n/ac stations using different bandwidths. The rest of the 20 MHz channels are called secondary channels. On the primary channel, the legacy binary exponential backoff is performed as follows. After a Distributed Coordination Function (DCF) Inter-Frame Spacing (DIFS) period, a transmission-attempting device selects a backoff counter and waits for the counter to expire. Before the counter reaches zero, however, the station senses secondary channels for one Point Distribution Function (PCF) Inter-Frame Spacing (PIFS) period. When all the primary and secondary channels are idle, the station starts a transmission. However, if not all the secondary channels are idle, the station has two choices as shown in Fig. 2 [9], [11], [17], [18], [19]. In the case of static access, the station retries the entire channel by contending again. For dynamic access, the station transmits on the primary channel and only idle secondary channels that are adjacent to the primary channel. Of course, the merged channel should coincide with one of the channelizations in Fig. 1. The static access is mandatory, while the dynamic access is optional.
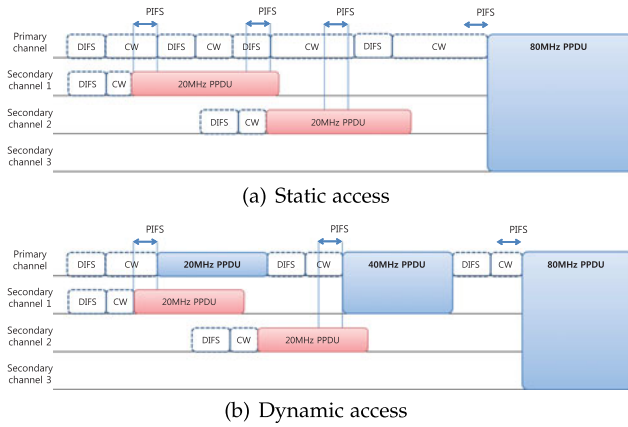
(a) Static access

(b) Dynamic access

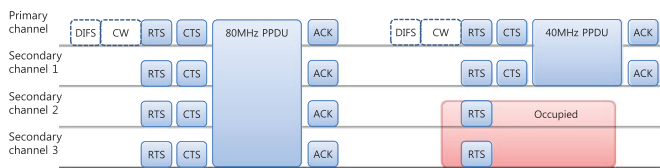Fig. 2. Static and dynamic channel accesses in 802.11ac.

Fig. 3. Enhanced RTS/CTS in 802.11ac.

To solve this, an *enhanced RTS/CTS*, which is optional, can be used for spectral and spatial reservations [9], [17], [18], [19]. A transmitter sends an Request-To-Send (RTS) frame for each 20 MHz-channel to reserve the entire channel to a receiver before transmitting a data frame as in the legacy RTS/CTS, which is shown in Fig. 3. The receiver checks idleness of each channel upon receiving the RTS frame, and then sends back a Clear-To-Send (CTS) frame after a Short Inter-Frame Spacing (SIFS) period. Other devices that heard either an RTS or CTS frame, regard the corresponding channels busy and defer their transmissions on those channels for the Network Allocation Vector (NAV) duration specified in the RTS/CTS frame.

The enhanced RTS/CTS can be used along with the dynamic access as shown in Fig. 3. But it was designed to solve the hidden terminal problem which is originated from the physical location discrepancy of a transmitter and a receiver. We need a new solution for the HC problem since the RTS/CTS messages can also suffer the HC problem.

2.2 Effect of Bandwidth Selection

Fig. 4 shows Modulation and Coding Scheme (MCS) levels and the corresponding receiver sensitivities defined in the 802.11ac specification. Receiver sensitivity is the minimum received signal power required for decoding a signal with the probability of greater than 90 percent. So, the required receiver sensitivity can be considered as an ideal measure of channel condition (i.e., determined by only path loss attenuation). Intuitively, a higher MCS level requires a higher receiver sensitivity for correct signal decoding.

As the figure shows, using a wider bandwidth with the same MCS level requires a better channel condition. On the other hand, from the perspective of achievable throughput, it is always best to use as large a bandwidth as possible. When the channel condition is -79 dBm, the viable options are MCS 1 at 20 MHz and MCS 0 at 40 MHz. The theoretical data rates under each option are 13 and 13.5 Mbps, respectively.
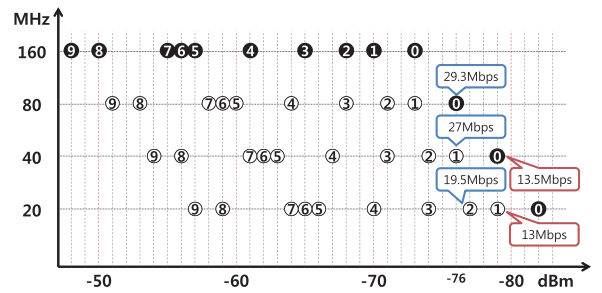

Fig. 4. Ideal MCS levels on each bandwidth according to receiver sensitivity, where the number inside each circle indicates the corresponding MCS level and the x-axis represents the required receiver sensitivity in decreasing order.

Likewise, if the channel condition is -76 dBm, there are three options, i.e., MCS 2 at 20 MHz, MCS 1 at 40 MHz, and MCS 0 at 80 MHz, with the data rates of 19.5, 27 and 29.3 Mbps, respectively. Therefore, in theory, using a wider bandwidth is always better on a single link. The best option for each receiver sensitivity is indicated by a black circle in Fig. 4.

On the other hand, using a wider bandwidth accompanies some disadvantages. First, it reduces the transmission range. Since the transmission power is fixed due to the restriction at the power amp hardware, using a wider bandwidth lowers power spectral density of each transmission. For instance, if 100 mW is used for transmission, then 5 and 2.5 mw/MHz are the power spectral densities for 20 and 40 MHz bandwidth, respectively.

Second, using a wider bandwidth makes the spatial reservation range relatively smaller, so it is less likely to affect others' transmissions. For this reason, secondary channels can be used more aggressively with a less sensitive CCA threshold, i.e., higher CCA threshold value, for channel assessment. This has led the standardization to use different CCA sensitivities for primary and secondary channels.

The first disadvantage intrinsically implies the second one. The transmission range on a wider bandwidth becomes shorter, thus reducing the spatial area that the transmitter reserves via CSMA/CA. So, if there is another device outside the reservation range of a transmitter, the packet in transmission may experience a potential interference. This problem did not happen until 802.11ac was introduced, because all the devices used the same bandwidth and power until then.[1] However, in 802.11ac with non-overlapping channelization, the use of heterogeneous bandwidths ranging from 20 to 160 MHz causes an imbalance between medium reservation capabilities [12], [15].

In summary, the bandwidth selection needs to balance between throughput performance and robustness to potential interferences. Using a larger bandwidth leads to a higher data rate thus reducing the transmission time at the expense of shortening the transmission range. The same finding was reported in [12], [15]; especially, similar findings from experiments within 802.11n systems in [12].

3 HIDDEN CHANNEL PROBLEM

Next we describe the HC problem originated from the discrepancy between reservation and sensing capabilities.

---

1. 802.11n also has the same problem, but it was not exposed because the maximum allowed bandwidth is only 40 MHz.

(a) Partial interruption
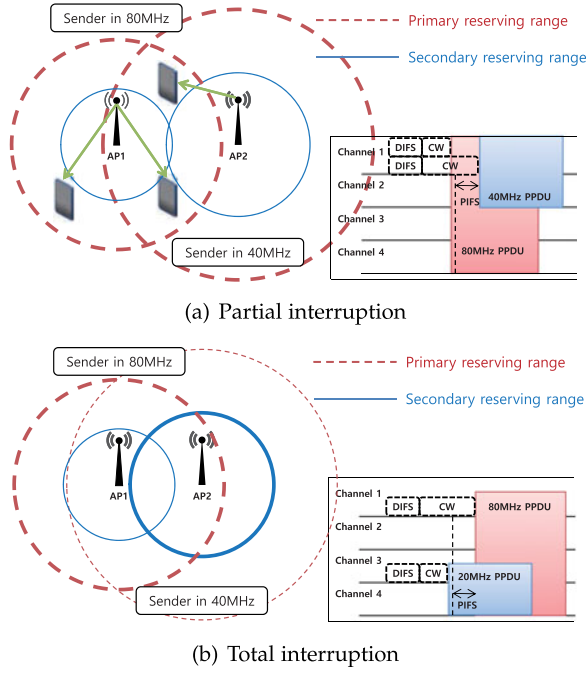

(b) Total interruption

Fig. 5. Hidden channel collision with the allocated channel numbers from AP1's perspective.

This problem has been articulated and analyzed in [11]. For completeness, we briefly summarize problematic situations in the following section, then present our experimental results to show that the problem is real followed by a simple probabilistic analysis showing the severeness of the problem in a network.

3.1 Problem Description

We use a simple channel model

$$PL(d) = 20 \cdot log\left(\frac{4\pi d_0}{\lambda}\right) + 10\alpha \cdot log\left(\frac{d}{d_0}\right), \qquad (1)$$

where α is the path-loss exponent and set to 3, d is the distance between a transmitter and a receiver, d_0 is the reference distance which is set to 1 m, and λ is the wavelength of 5.3 GHz. We use the transmission power of 17 dBm.

As mentioned before, 802.11ac defines two different CCA sensitivities for primary and secondary channels. For 20 and 40 MHz bandwidths, the primary channel sensitivities are -82 and -79 dBm, respectively, while the secondary sensitivities are -72 dBm. The primary and secondary sensitivities for 80 MHz bandwidth are -76 and -69 dBm, respectively [9]. Note that the primary sensitivity is for decoding incoming packets, while the secondary sensitivity is for detecting energy density.

Fig. 5 illustrates the HC problems caused by the discrepancy between CCA sensitivities [11], [17], [18], [19]. There are two APs in the figure: AP_1 occupies an entire 80 MHz channel while AP_2 uses a 40 MHz channel.

According to the channel model and two different CCA sensitivities, the reserving distance for each bandwidth can be calculated. There are two types of 'reserving' transmitter. If a reserving transmitter uses the primary channel of a sensing transmitter, it is called *primary reserving*. Note that the primary reserving is done with a more sensitive

TABLE 1
Reserving Distance for Each Bandwidth and Sensing Channel Type Calculated According to the Channel Model and CCA Sensitivity

Bandwidth (MHz)	Primary distance (m)	Secondary distance (m)
20	54	25
40	43	20
80	34	16
160	27	13

threshold. The other case happens when the reserving transmission occupies only the secondary channel(s) of the sensing transmitter. This is called *secondary reserving*. In other words, based on the CCA sensitivity and energy level of the transmission, there are two reserving ranges, *primary* and *secondary reserving ranges*. Table 1 shows the calculated distances which depend on the channel model and each CCA sensitivity threshold. These example values will be used throughout the paper for an illustrative purpose.

In Fig. 5, we represent transmitters as APs and receivers as devices. There may be a conflict between two transmission-attempting links, i.e., transmitter-receiver pairs. Dotted and solid circles in the figure represent reserving ranges with the primary and secondary sensitivities, respectively. AP_1's ranges are shorter than AP_2's since AP_1 uses a wider bandwidth than AP_2. Depending on channel configurations of the two APs, only one of the two reserving ranges is activated for each AP. The activated reserving ranges are illustrated with bold lines in the figure.

Fig. 5a illustrates the HC problem in which a smaller bandwidth transmission interrupts a larger one. Since part of the larger bandwidth is interrupted, it is called *partial interruption*. In this case, AP_1 is within the primary reservation range of AP_2 while AP_2 is outside that of AP_1. Therefore, AP_1 can sense the transmission from AP_2 with the primary sensitivity on channel 1. When AP_1 starts to transmit after channel acquisition through contention, AP_2 regards channels 1 and 2 as idle, and starts transmission, thereby resulting in a collision.

Fig. 5b illustrates another HC problem, where the larger bandwidth channel interrupts the smaller one. This is called *total interruption* since the entire bandwidth of the smaller bandwidth channel is interfered with by the wider one. Because AP_2 occupies only secondary channels of AP_1, AP_2 reserves channels with the secondary reserving range. So, AP_1 cannot sense the existence of AP_2's transmission by the secondary sensing range which leads to a collision in the opposite direction. We call both *partial interruption* and *total interruption*, respectively, in this paper.

The static and dynamic access mechanisms illustrated in Fig. 2 suffer from the HC problem due to heterogeneous carrier sensing capabilities. If there exists an HC problem, an already acquired channel through CCA and contention is not immune from potential interference. That is, the result of CCA is not reliable in both access mechanisms. A transmitter's decision on whether to transmit and/or which channels to use can be wrong in such cases. Again, the enhanced RTS/CTS in Fig. 3 cannot solve the HC problem since RTS/CTS control messages can also suffer the HC
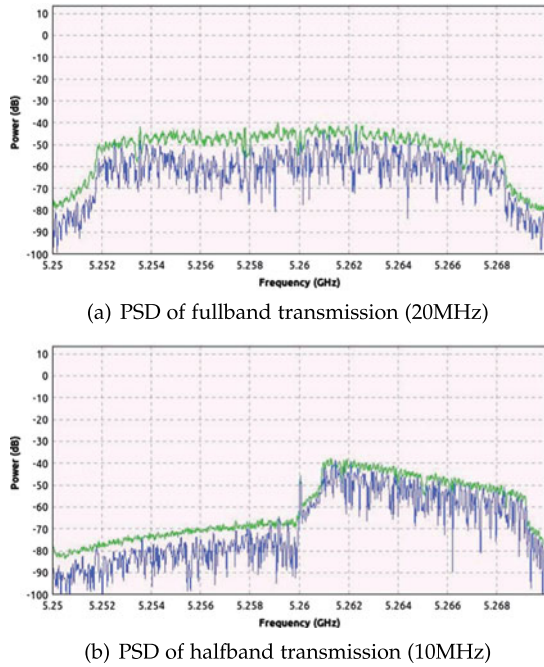
(a) PSD of fullband transmission (20MHz)

(b) PSD of halfband transmission (10MHz)

Fig. 6. Power spectral density of full and half band transmissions.

(a) Topology 1

(b) Topology 2

(c) Topology 3

(d) Topology 4

Fig. 7. Experimental topologies.

problem. The control messages over wider bandwidth channels suffer from lower power spectral density, thus shortening their spatial reserving distance. Also, even with a successful RTS-CTS handshaking, RTS or CTS messages are oblivious to the potential interferer if the hidden channel problem exists. Despite the ability to deal with the spatial reserving asymmetry, the enhanced RTS/CTS is not suitable for solving the HC problem.

Of the many issues being considered by the 802.11ax Task Group (TG) [8], dynamic CCA sensitivity control is drawing significant interest from researchers. The advance of hardware technologies has made it possible to adjust CCA sensitivity according to certain conditions. The major goal of dynamic CCA control is to improve efficiency of spatial and spectral reuse. So, we consider both cases of with and without the discrepancy between CCA sensitivities. The HC problem condition still holds without this discrepancy because of varying power spectral density.

3.2 Experimental Results

We have conducted simple experiments to show that the HC problem is real. We used USRP N200 with GnuRadio [2], [3] and WARP v.3 with WARPLab reference design version 7.5.1 [1]. The WARP v.3 uses MAX2829 transceiver hardware [4]. The ADC and DAC in MAX2829 have an intrinsic function for converting Received Signal Strength Indicator (RSSI) values from the hardware to digital values, which is similar to

$$RSSI(dBm) = (200/3069) \cdot RSSI_D - c$$
$$c = \begin{cases} 280/3 & \text{gain = high} \\ 155/2 & \text{gain = medium} \\ 126/2 & \text{gain = low,} \end{cases} \quad (2)$$

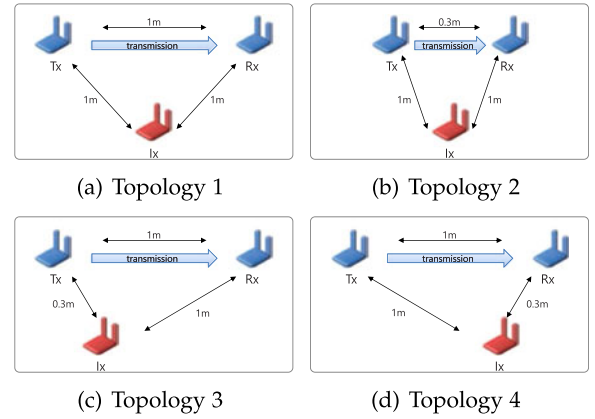where $RSSI$ has the unit of dBm and $RSSI_D$ is the digitized RSSI value the ADC returns.

First, we measure the difference in spectral density for 10 and 20 MHz transmissions with a fixed power to verify the idea that reducing bandwidth in half doubles power spectral density. A WARP board transmits a packet, and its spectral density is measured by a USRP board which is 0.5 m away from the transmitter. Since the stably supporting bandwidth of the WARP board is 20 MHz at 5 GHz band,[2] we use 20 MHz for a full band transmission and 10 MHz for a half band one in the following experiments without loss of generality. Both interpolation [14], [15] and subcarrier nulling [16] were used to control bandwidth, and yielded the same results.

Fig. 6 plots the power spectral density (PSD) while varying the bandwidth, where each fluctuating line at the lower side is the PSD at a specific point in time, and each slightly fluctuating line at the upper side is a peak holding graph that stores the maximum PSD over time. As shown in the figure, the PSD with the full bandwidth is around −45 dBm while that with a half bandwidth is approximately −40 dBm. This result simply verifies that an approach using a smaller bandwidth concentrates the entire power on the narrow bandwidth, which results in higher PSD than that of using a wider bandwidth.

We now consider the dependency of channel assessment on physical locations of a transmitter, a receiver and an interferer. Fig. 7 shows the topologies used in experiments where 3 WARP boards are used to create a simple transmitter-receiver (Tx-Rx) pair with an interferer (Ix). Topology 1 is for an equal distance scenario, topology 2 for a close Tx-Rx scenario, topology 3 for a close Tx-Ix scenario, and topology 4 for a close Rx-Ix scenario. The Tx-Rx pair use full bandwidth and the Ix occupies only a half of the bandwidth. The Tx and Ix transmit simultaneously to acquire CCA results and bit error rates. The averages with the standard deviation bars are shown in Fig. 8, where each result is obtained from 100 repeated measurements.

Fig. 8a shows the CCA results for different topologies, where the conventional CCA is performed right before starting a transmission and then the post-CCA, which will be detailed in the next section, is executed after completing a transmission. The conventional CCA results at both Tx

---

2. A WARP hardware supports up to 40 MHz bandwidth. However, when a packet is sent over 40 MHz bandwidth at 5 GHz using the WARPLab reference design, it suffers from a higher bit error rate.
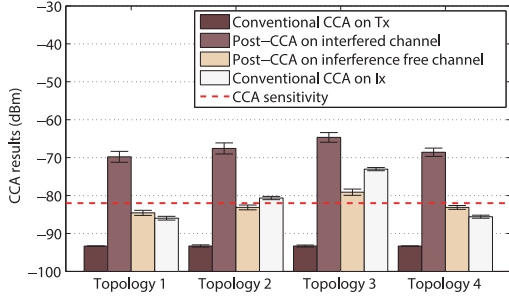
(a) Conventional CCA and Post-CCA results on both of half bandwidth channels at Tx, and CCA results at Ix while Tx is transmitting
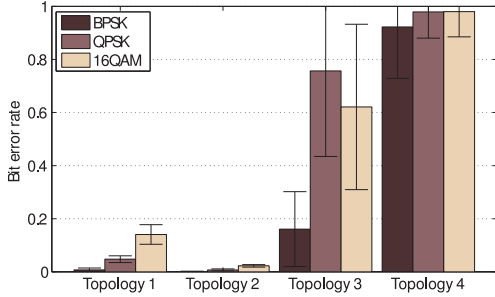
(b) Bit error rates of BPSK, QPSK and 16QAM modulations on each topology when there is a hidden channel interference

Fig. 8. Experimental results for various topologies.

and Ix are shown with the post-CCA results on both of half bandwidth channels.

As shown in Fig. 8a, the post-CCA result values on the interfered half bandwidth channel are much larger than those on the other interference-free one. This is a simple, expected result since the interference occupies only half of the channel. The post-CCA results on the interference-free half-channel should be similar to the conventional CCA results, which are nearly -90 dBm in the experiment. However, in Fig. 6b, there is power leakage on the interference-free half channel due to the imperfection of bandwidth control software and hardware. Albeit with the imperfection, these results suggest that the post-CCA can be useful in detecting the HC collision.

Note that conventional CCA results at the Ix side during the Tx's transmission are also different from post-CCA results at the Tx side. This gap implies unbalanced CCA capabilities of Tx and Ix. The dotted line in Fig. 8a represents the primary CCA sensitivity level, i.e., -82 dBm. Above (below) the sensitivity level is the region for channel busy (idle). During the Tx's transmission, Ix cannot detect the existence of a transmission on topologies 1 and 4. However, on the same topologies, Tx is aware of the existence of Ix's transmission through the post-CCA results on the interfered half channel. This implies that Ix interferes with Tx all the time on the half channel due to the failure in detection of channel's busyness. That is, the HC problem occurs.

The corresponding bit error probabilities are plotted in Fig. 8b when Ix interferes with Tx. Since bit error rates (BER) without interference are nearly zero on all the topologies, observed bit errors are caused by Ix's transmission. As shown in the figure, the severity of the problem depends on the modulation level. Transmissions at a higher modulation level—used when the channel condition is

good—are more prone to errors due to the interference. These experiments show the discrepancy between the CCA capabilities of different bandwidths, and also reveal that the discrepancy and physical topology affect transmission bit error rates greatly.

In [11], the impacts of the HC problem on throughput and packet error rate are analyzed with Markov chain modelings. Different from this, our BER measurements give more realistic impacts of the HC problem on the error rate. Depending on the topology, the HC problem can cause nearly 100 percent bit error rate or packet error rate.

3.3 Analytic Results

The previous experiments show that the HC problem exists on a link topology. The next question is how severe the problem is in a network topology. To see this, we take a probabilistic approach for a network where nodes are distributed uniformly. Applying different distributions is straightforward, however we use the uniform for simplicity.

The probability of suffering the HC problem for a link (transmitter-receiver pair) when using bandwidth bw can be expressed as

$$Pr_n^{HC}(bw) = \sum_{BW \neq bw} Pr_n^{spatial}(bw, BW) \cdot Pr^{spectral}(bw, BW), \quad (3)$$

where BW is the bandwidth of a potential interferer, n is the channel attenuation factor. For a particular BW, the probability of HC suffering is the product of the probabilities of HC in spatial and spectral sufferings. $Pr_n^{spatial}(bw, BW)$ is the probability that the interferee and interferer are located to suffer the HC problem in spatial topology, and $Pr^{spectral}(bw, BW)$ is the probability that the interferee and interferer use an HC suffering bandwidth-channel configuration given that they are located within the HC suffering distance. Summing up all possible BWs, we can drive the average probability of HC suffering as Eq. (3)

$$Pr_n^{spatial}(bw, BW) = \begin{cases} pos\left(\frac{r_p^n(BW) - r_s^n(bw)}{r_p^n(BW)}\right) & \text{if } bw < BW \\ pos\left(\frac{r_p^n(BW) - r_p^n(bw)}{r_p^n(BW)}\right) & \text{if } bw > BW \\ 0 & \text{otherwise,} \end{cases} \quad (4)$$

$$pos(x) = \begin{cases} x & \text{if } x \geq 0 \\ 0 & \text{otherwise,} \end{cases} \quad (5)$$

$$r_{reserving}(bw, \theta) = 10^{\frac{17 - 3\frac{bw}{20} - 20 \cdot log(\frac{4\pi}{\lambda}) - \theta}{10 \cdot \alpha}}. \quad (6)$$

Eq. (4) calculates the area with the reserving range discrepancy over the entire transmission area for the total HC (first row) and partial HC (second row), assuming a simple circle or sphere transmission area model, where $r_p(\cdot)$ and $r_s(\cdot)$ are the primary and secondary reserving ranges. Using Eq. (6) derived from Eq. (1), we calculate the reserving ranges for the sensitivity θ. Therefore, we have $r_p(bw) = r_{reserving}(bw, -82)$ and $r_s(bw) = r_{reserving}(bw, -79)$. We use $n = 3$ for a 3-dimensional space. If the input parameter is BW, they express the range for an interferer and bw for an interferee, respectively. The discrepancy of the area or volume is the probability of the HC problem in spatial
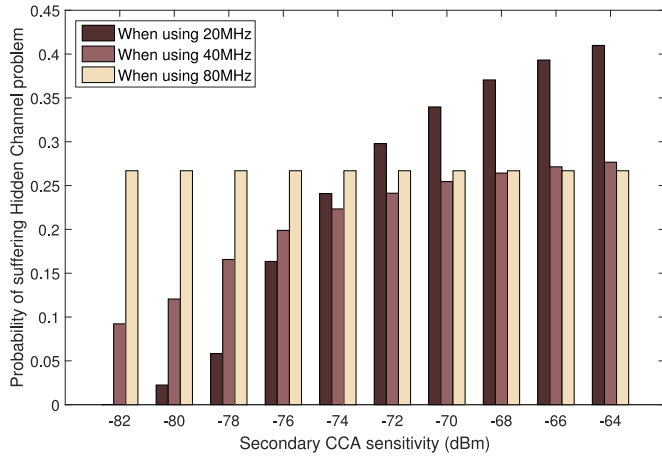
Fig. 9. HC suffering probability as a function of bandwidth and secondary sensitivity.
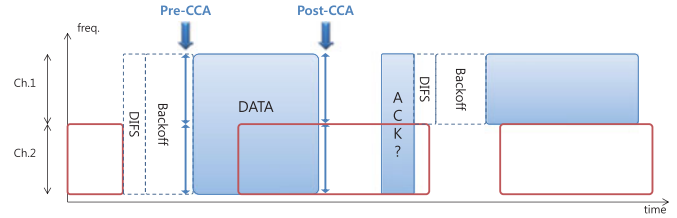

Fig. 10. Post-CCA operation.

positioned to suffer the hidden channel problem. Their conclusion is that the HC problem happens with 50 percent of probability in time-domain. Combining these results, we can see that roughly 10 percent of collisions are due to the hidden channel problem. So, reducing the probability of HC can make a performance improvement. In what follows, we propose a remedy for the problem.

4 POST-CCA

The intuition behind PoBA is that an 'interferee' can sense its 'interferer', but not vice versa, and hence the interferee should avoid collision. Fig. 10 illustrates the post-CCA operation in a simple two-channel scenario, where filled solid squares represent the interferee's channel occupancy and empty solid squares represent the interferer's.

The interferee using the entire channel starts to back off right after the interferer finishes its transmission. Upon sensing the entire channel idle, the interferee starts transmission. The interferer also transmits its own since it is unable to sense the channel busy. With the post-CCA operation, the interferee is aware of the existence of a disrupting transmission on channel 2. Since no ACK packet is received in time, the interferee concludes that its transmission failed due to an HC collision.

Table 2 shows interferee's speculation about the network condition according to the observations from post-CCA about idleness of used channels and whether an ACK packet is received correctly. The case of our interest is when a post-CCA result is busy without an ACK reception. The other cases are usual as in homogeneous bandwidth networks.

If the interferer's transmission ends before the interferee's, the post-CCA cannot detect the interferer's existence. Clearly, the duration of the interferer's transmission affects the performance of the post-CCA operation. If its duration is relatively short, a transmission failure will be considered as a channel fading error. We leave this case to the responsibility of Auto Rate Fallback (ARF) and Forward Error Correction (FEC) both of which are designed to combat bad channel conditions.

After finishing a transmission, the transmitter switches its antennas from transmitting to receiving mode to wait for

dimension. Note that if the allocated bandwidths are the same or the area for the interferee is larger than that for the interferer, the HC problem does not happen.

Then by enumerating all the possible channel configuration cases, we can derive the spectral HC probability on average as Eq. (7), assuming they are positioned to suffer HC problem.[3] In this equation, an arrow head directs interferee and its tail is for interferer

$$
Pr^{spectral} = \begin{cases} 0.25 & \text{if } 20 \leftarrow 40 \\ 0.75 & \text{if } 20 \leftarrow 80 \\ 0.25 & \text{if } 40 \leftarrow 20 \\ 0.5 & \text{if } 40 \leftarrow 80 \\ 0.25 & \text{if } 80 \leftarrow 20 \\ 0.5 & \text{if } 80 \leftarrow 40 \\ 0 & \text{otherwise.} \end{cases} \tag{7}
$$

Using the above equations, we can calculate the average probability of HC suffering, and Fig. 9 shows the results. Here, the probabilities are calculated as a function of (i) bandwidth and (ii) secondary sensitivity. In the figure, the primary sensitivity is fixed to -82 dBm. If the secondary sensitivity is the same as the primary, only the bandwidth (power spectral density) affects the existence of the HC problem, not channel configuration. Therefore, only partial HC happens. As the secondary sensitivity increases, total HC appears and gets severer. This tendency is shown in the figure for 20 and 40 MHz cases. Since a 20 MHz link has more chance to suffer total HC (from 40 and 80 MHz) than a 40 MHz link (only from 80 MHz), the HC probability for 20 MHz increases more sharply. However, the HC probability for 80 MHZ remains the same since the 80 MHz link only suffers from partial HC in which only the primary sensitivity matters.

Roughly, the probability of HC suffering is around 20 percent regardless of the allocated bandwidth in a random topology. And actual packet collision depends on contention parameter values and the length of each packet [11]. They presented the severity of the problem on the performance through a time domain analysis, which is "collision rate versus contention window", assuming that links are

---

3. We skip the enumeration.

TABLE 2
Post-CCA Observations and Intuitions

Observation		Intuition
Post-CCA	ACK?	
Idle	Yes	Working well
Idle	No	Fading error/Hidden terminal
Busy	Yes	Collision but working well
Busy	No	Hidden channel collision error

an ACK packet. This means that performing a post-CCA operation is not new, but the conventional operation has not yet made use of the information available. It has not been used since spectral reservation (not spatial) was assumed to work well in homogeneous bandwidth networks. In this sense, the post-CCA is standard compliant and does not require any new operation.

Conceptually, the post-CCA operation helps a transmitter assess the network condition, like CSMA/CD in the wired Ethernet where a transmitter can detect other signals during its own transmission. In wireless networks, collision detection is not possible during transmission. But our post-CCA helps improve assessment of channel condition by sensing the channel once again after completing a transmission. Although the post-CCA operation and CSMA/CD are different, they share a similar concept of re-assessing channels after/during a transmission. Next we propose a bandwidth adaptation (PoBA) algorithm to alleviate the HC collision problem. CSMA/CD aborts transmission if a collision is detected. However, a different approach should be taken in wireless systems since no other action can be taken during a transmission.

5 PoBA

POMDP is a type of reinforcement machine learning. Since it can be applied to our problem, we first briefly summarize it for better understanding and illustrate that the HC problem has partial observability in this section. Then we elaborate on *PoBA* modeling and a bandwidth-channel adaptation scheme that exploits information from post-CCA operation, followed by an illustrative example.

5.1 POMDP

POMDP is a tool for planning and acting in a partially observable stochastic domain; given a complete and correct model of the world dynamics and a reward structure, it helps to find a way for optimal behavior [26].

A partially observable Markov decision process (MDP) can be described as a tuple $\langle S, A, T, R, \Omega, O \rangle$ [26], where

- S is a finite set of states of the world;
- A is a finite set of actions;
- $T : S \times A \to \Pi(S)$ is the *state-transition function*, which gives a probability distribution over world states for each world state and agent action. Here $T(s, a, s')$ represents the probability of ending in state s', given that the agent starts in state s and takes action a;
- $R : S \times A \to \mathbb{R}$ is the reward function, which gives the expected immediate reward gained by the agent for taking an action in each state. $R(s, a)$ represents the expected reward for taking action a in state s;
- Ω is a finite set of observations that the agent can experience of its world; and
- $O : S \times A \to \Pi(\Omega)$ is the *observation function*, which gives a probability distribution over possible observations for each action and its resulting state. $O(s', a, o)$ represents the probability of making observation o given that the agent took action a and landed in state s'.
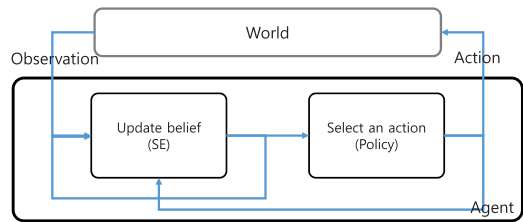

Fig. 11. A POMDP model. The POMDP agent can be decomposed into a state estimator (SE) and a policy.

Fig. 11 shows how POMDP agent works in two parts: observing action and generating action. The agent keeps an internal probability distribution over S, called *belief state*, b. The component of *state estimator (SE)* is responsible for updating belief state based on the last action, the current observation, and the last belief state. And the *policy* component generates an action to take based on the updated belief state.

The belief state, a probability distribution over entire possible states of the world, provides agent information about the world in a probabilistic manner. It is because our agent only infers its state through observations. In other words, the agent cannot know the exact state of the world directly. Then based on the belief state, the agent chooses an action among A which is expected to produce an optimal reward in some manner.

The world of our interest generates an observation based on the action (a) chosen by the agent, and its internal state (s) and landing state (s'). Then the observation is fed to the agent for the next iteration. While the state transition follows the state-transition function T, the observation-generation follows the observation function O. The transition model is given but the exact state of the world is hidden to the agent. The belief state is updated by Eq. (8).

In the equation, $b(s)$ denotes the probability assigned to world state s by belief state b. Naturally, $0 \le b(s) \le 1$ for all $s \in S$ and $\sum_{s \in S} b(s) = 1$. The state estimator computes new belief state b', given old belief state b, action a, and observation o. The new belief state can be obtained from the basic probability theory.

The belief state comprises a sufficient statistic for the past history and the initial belief state. That is, given the current belief state, no more information about its past actions and observations would increase the expected reward by providing more data [26]. So, the belief state is Markovian. If we consider belief as a state, then the POMDP can be reduced to an MDP which can be described with a tuple $\langle S, A, T, R \rangle$

$$
\begin{aligned}
b'(s') &= Pr(s' \,|\, o, a, b) \\
&= \frac{Pr(o \,|\, s', a, b) Pr(s' \,|\, a, b)}{Pr(o \,|\, a, b)} \\
&= \frac{Pr(o \,|\, s', a) \sum_{s \in S} Pr(s' \,|\, a, b, s) Pr(s \,|\, a, b)}{Pr(o \,|\, a, b)} \quad (8) \\
&= \frac{O(s', a, o) \sum_{s \in S} T(s, a, s') b(s)}{Pr(o \,|\, a, b)}.
\end{aligned}
$$

There are many types of POMDP modelings and solving techniques depending on how a problem is defined, for example, how the rewards are accumulated as time passes. We then seek to apply POMDP to our bandwidth-channel adaptation problem by exploiting the partial observability of post-CCA.
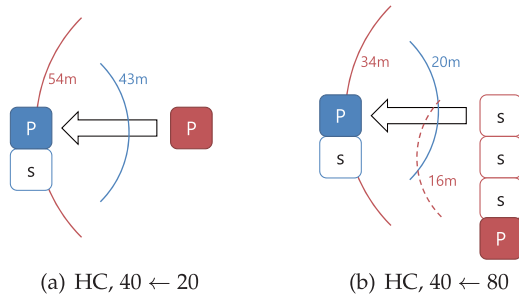
Fig. 12. Partial observability of HC problem. In the both cases, the interferee's post-CCA results for the upper and lower channels are 'Busy' and 'Idle', respectively.

5.2 Partial Observability of HC

Before jumping into our problem modeling, we illustrate the partial observability characteristics of post-CCA to justify the application of POMDP, not MDP. Fig. 12 shows an illustrative example of partial observability with post-CCA. In the figure, the bandwidth of the interferee is 40 MHz and for illustrative purposes, we use the simple distance interpretation of HC problem as in Section 3.1.

First, consider the case of partial HC as in Fig. 12a. Since they both are primary reserving, their reserving ranges are 43 and 54 m respectively. When they are positioned between these ranges, a partial HC problem happens. The post-CCA result on the interferee when suffering HC is 'Busy' on the first channel and 'Idle' on the second, because there is no transmission on the second channel from the interferer.

Now, consider the case of Fig. 12b. In this total HC case, the interferee is secondary reserving while the interferer is primary reserving. Their reserving ranges are then 20 and 34 m, respectively. So, again, when they are positioned between these ranges, a total HC problem happens. On the primary channel the post-CCA result is 'Busy' because the interferer's primary reserving range is 34 m. However, on the secondary channel, the interferer is secondary reserving and its range is 16 m. Therefore, the post-CCA results on the channels are 'Busy' and 'Idle', the same as the previous case.

Therefore, with the result from the post-CCA, the interferee can infer that there is an interferer which is either of the two. This is exactly what partial observability means in POMDP. Our interferee, the agent in POMDP, cannot know the exact type of the interferer. It can only infer that a number of interferer types exist.

Generalizing the partial observability in our HC problem, we enumerate all possible HC cases, and show the results in Table 3. In the table, the rows are for interferee and the columns are for interferer. And 20, 40, and 80 represent the bandwidth and 1, 2, 3 and 4 represent the location of the primary channel. A combination of the two represents a bandwidth-channel configuration. Assuming that the maximum bandwidth is 80 MHz, there are 12 possible configurations in our problem.

Symbol '○' in the table indicates that when the interferee takes a configuration on the row and the interferer on the column, an HC problem can arise and it can be detected through post-CCA. So, for a bandwidth-channel configuration that the interferee can take, there are 3 to 4 possible potential interferers and the interferee cannot distinguish

TABLE 3
The HC Existence and Detection Possibility for an Interfer*ee* to Detect the Existence of an Interfer*er* through the Post-CCA Operation

ee	er	20				40				80			
		1	2	3	4	1	2	3	4	1	2	3	4
20	1						○			○		○	○
	2					○					○	○	○
	3								○	○	○	○	
	4							○		○	○		○
40	1	○										○	○
	2		○									○	○
	3							○		○	○		
	4								○	○	○		
80	1	○				○	○						
	2		○			○	○						
	3							○				○	○
	4								○			○	○

Numbers 1 through 4 represent the location of the primary channel. 'Possible' is represented with '○', and not possible otherwise.

between them. This justifies why POMDP, not MDP, should be applied to our problem.

5.3 POMDP Modeling for PoBA

We apply POMDP to model our PoBA in this section. From the definition of POMDP, $\langle S, A, T, R, \Omega, O \rangle$ need to be defined in our bandwidth-channel adaptation problem. As before, we assume the maximum bandwidth of 80 MHz for brevity.

First we define state s as an array of 12 bits, where each element is either 0 or 1. The bit '1' indicates that there exists at leat one potential interferer which uses the bandwidth-channel configuration corresponding to the bit position in the array, and otherwise '0'. The order of bandwidth-channel configuration is the same as the order on the row or column in Table 3. For example, if the first element is 1, there is at least one potential interferer using 20 MHz bandwidth with primary channel 1. And if the last element is 0, then there is no interferer using 80 MHz with primary channel 4. So, there are 2^{12} possible states, and which set is denoted as S.

Naturally, an action $a \in \{a_1, a_2, \ldots, a_{12}\}$ is one of the 12 bandwidth-channel configurations and the set of all the available actions is denoted as A. However, a link may only utilize a subset of A, due to the limitation of the protocol version (802.11 a/b/g/n) or the distance between the transmitter and the receiver. If the link uses 802.11n, only transmissions of 20 and 40 MHz are allowed. So, there are 8 action choices. Or if the receiver is at the edge of the transmission range of the transmitter, only 20 MHz transmission with the lowest MCS level is possible as in Fig. 4.

The observation set Ω has only two elements: *HC and no HC*. An observation is obtained through the post-CCA operation. Only collisions on the primary channel can be observed because of the partial observability characteristic. Then the observation function $O : S \times A \rightarrow \pi(\Omega)$ can be induced from Table 3 as follows. Given a state s (column of the table) and an action a (row of the table), if the ith bit is '1', we know there exists some interferer(s) but we don't know how many. Then an HC event can be observed.
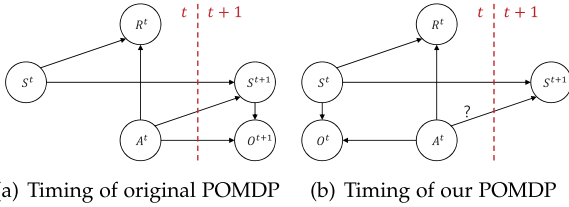
(a) Timing of original POMDP   (b) Timing of our POMDP

Fig. 13. A modification on the timing of POMDP to fit our problem.

TABLE 4
Partial Observability within 40 MHz Bandwidth

ee	er	20		40	
		1	2	3	4
20	1				○
	2			○	
40	3	○			
	4		○		

A difference between the original POMDP model and ours is the timing that an observation is generated. Fig. 13 illustrates the timing difference. In the original POMDP, an observation is generated after the world changes its state in $t + 1$. But in our formulation, after choosing an action (bandwidth-channel configuration), the agent transmits a packet, and whether the packet transmission suffers from HC problem or not can be observed. Then the state of the world may change according to the action that the agent has taken. So, in Fig. 13b, an observation is generated in t, and the state of the world changes from S^t to S^{t+1}.

The agent is not able to detect whether the agent's action has incurred state transition in our problem. This means that since the HC problem can be detectable at the interferee's side only, it is vague whether A^t has caused transition from S^t to S^{t+1}. Therefore, our model adopts the belief update consisting of two steps.

The first step, as shown in Eqs. (9) and (10), updates belief assuming no state transition of the world. And the second step is for a simple random transition, which is modelled as Eq. (11). The first step reflects that an observation is made in the current time period, and the second step represents a vague state transition of the world. Due to the vagueness, we adopt a simple transition model where each bit of the state vector inverts itself with a predefined small probability (for example, 0.1 in our simulation setting)

$$b'(s') = \frac{O(s', a, o) \sum_{s \in S} T^{noTransition}(s, a, s') b(s)}{Pr(o \,|\, a, b)} \quad (9)$$

$$T^{noTransition}(s, a, s') = \begin{cases} 1 & \text{if } s' = s \\ 0 & otherwise \end{cases} \quad (10)$$

$$b''(s'') = \sum_{s' \in S} Pr^{transition}(s'' \,|\, s') b'(s'). \quad (11)$$

Lastly, the reward function is modeled as a function of bandwidth and the existence of HC problem. Recall that using wider bandwidth helps to achieve more theoretical throughput. But if HC exists, throughput will be degraded. So, $T^{expected}_{a_i} = \alpha \times bandwidth \times \beta_{HC}$, where α is an arbitrary constant and $0 \le \beta_{HC} \le 1$ reflects the fraction of the throughput under HC suffering condition. The defined reward function is used for selecting an optimal action given a belief state. When deciding, the *Policy* entity calculates the expected throughput on each action from the available action set, i.e., the subset of actions that the link can choose from.

Since we only have 12 actions available, the POMDP algorithm may not converge to a single bandwidth-channel configuration if there are more than 12 potential interferers, each affecting each of the actions. This is basically a complicated

version of a distributed coloring problem with a limited number of colors and with types of edge varying depending on a selected color on vertices. We leave more solid analysis of the convergence of the algorithm for future work.

5.4 PoBA Example in Total 40 MHZ

In this section, we present an example of simple operation of PoBA within a maximum bandwidth of 40 MHz. An action is $a \in \{a_1, a_2, a_3, a_4\}$, where a_1 and a_2 are 20 MHz with primary channel 1 and 2, while a_3 and a_4 are 40 MHz with primary channel 1 and 2 , respectively. Since the number of actions is 4, the number of states is 16. So we have a state $s \in \{s_1, \ldots, s_{16}\}$ where $s_i = \{s_i^1, s_i^2, s_i^3, s_i^4\}$. s_i^j is 1 if there exists a potential interferer using a_j, and 0 otherwise. The orders for s_i ($i \in 1, \ldots, 16$) are assigned in an increasing order, i.e., $0000, 0001, \ldots, 1111$.

For the observation function used in this example, post-CCA events are summarized in Table 4. Note that this table is a subset of Table 3. The bit transition probability for the state-transition function is set to 0.1 and β_{HC} is set to 0.5. Additionally, we adopt another parameter called 'HC observation probability', and set it to 0.5 to reflect the chance of observing HC through post-CCA.

The initial belief state the agent has is set to $16 \times \{0.0625\}$, which means the agent has no prior knowledge regarding the state of the world. Then the agent takes an action a_4, which the *Policy* entity returns, owing to the largest expected reward. If there is a potential interferer that interrupts our agent and it is observed through post-CCA, *SE* will update the belief as $4 \times \{0.0125, 0.0125, 0.1125, 0.1125\}$. This is because from Table 4, a potential interferer is anticipated to use a_2 and it corresponds to the second least significant bit in the state vector.

Then, the agent's *Policy* entity returns action a_3, which is anticipated to return the most largest reward under the update belief. Taking the action, the agent again detects HC, and the updated belief becomes $4 \times \{0.0045, 0, 0045, 0.0205, 0.1845\}$. Also, from the table, the agent can infer that there are other potential interferers using action a_1. Thus the states with both the least and second least significant bits of 1 (i.e., $xx11$ where x is either 0 or 1) get the highest probability.

Because of the random transition probability, all the elements in the belief vector never become 0. The vagueness of the transition in the model always assigns some non-zero probability to the elements of each state.

The example presented here can be easily extended to the case with 80 and 160 MHz. However, as the bandwidth increases, the number of possible states increases exponentially. This is a drawback of the POMDP model.
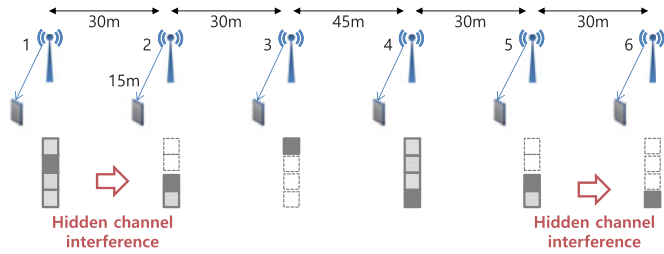
Fig. 14. 6-chain topology for simple simulation.

6 EVALUATION RESULTS

We implemented a simulator for *PoBA* in C++. The performances in terms of packet error rate, throughput, channel utilization[4] and throughput fairness are measured with and without PoBA when closed loop channel estimation (i.e., explicit channel feedback) is applied.

Also, to see the effect of Auto Rate Fallback, a simple ARF rule is used along with *PoBA* for the case of open loop (i.e., no explicit channel feedback) systems. The simple ARF scheme decreases the MCS level by one when a packet error is detected twice in a row, and increases it if n_{succ} consecutive transmissions are successful, where we set $n_{succ} = 20$. We have tested two bandwidth-adaptation-aware ARF schemes: *conservative* and *aggressive*. Based on Fig. 4, we can think of two options for rate adaptation when bandwidth change occurs. For example, when the bandwidth switches from 40 to 20 MHz and the channel condition is -69 dBm, rates 3 and 4 are the options. Rate 3 before the bandwidth switch indicates that the channel condition is between -68 to -71 dBm, theoretically. The *conservative* scheme assumes the worst condition, i.e., -71 dBm, and chooses rate 3 while the aggressive one chooses rate 4 after the switch. Our simulation results show that the performance gap is marginal between the two schemes. Note that bandwidth adaptation is more macroscopic than rate adaptation. So, we use the conservative scheme in our simulation.

The slot time, DIFS, PIFS, and SIFS are set to $9, 34, 25$, and $16 \ \mu s$, respectively, and the transmission power is fixed at 17 dBm. We assume that the inter-transmission-attempting time is $100 \ \mu s$ and the packet size is 1,500 bytes. The transmission time depends on the selected MCS level and the number of control messages (i.e., RTS, CTS and ACK) with the PLCP (Physical Layer Convergence Protocol) overhead of $20 \ \mu s$. And we use the same contention window size as in 802.11 networks.

We considered the difference between the bandwidths that the interferee and the interferer are exploiting, so that the error rates of all the 20 MHz channels are averaged to obtain a single valued effective Packer Error Ratio (PER). Then, the effective PER is converted to effective SINR. The effective PER and SINR are calculated in the same way as in [24]. When calculating PER from SINR, we use the PER equation in [20] that counts various MAC-layer operations, such as MCS level, Viterbi algorithm, and packet size.

TABLE 5
Simulation Results for a Simple Topology in Terms of Error Rate (%), Throughput (Mbps), and Channel Utilization (%)

	No.	1	2	3	4	5	6
w/o PoBA	Err.	0.00	**81.20**	0.20	0.00	0.57	**56.41**
	Thr.	30.22	**0.53**	24.05	15.19	14.75	**2.74**
(closed)	Util.	43.62	**0.98**	55.51	18.61	49.16	**6.32**
w/ PoBA	Err.	0.42	**1.66**	0.61	0.65	1.89	**0.72**
	Thr.	22.76	**15.64**	23.36	14.66	18.72	**23.12**
(closed)	Util.	28.05	**29.14**	53.93	18.09	34.92	**53.38**
w/o PoBA	Err.	4.18	**3.96**	4.07	3.92	4.11	**3.79**
w/ ARF	Thr.	15.94	**10.76**	19.51	7.66	7.84	**6.10**
(open)	Util.	66.65	**44.69**	59.46	12.00	68.86	**53.06**
w/ PoBA	Err.	4.10	**3.34**	3.95	4.10	3.26	**3.88**
w/ ARF	Thr.	17.42	**15.98**	20.14	14.32	14.60	**17.84**
(open)	Util.	31.48	**39.59**	61.98	25.15	44.13	**57.61**

For PoBA, we have adopted the bit transition probability of 0.1 for each element in the state vector. We have tried different values for the probability, and found out that a value of smaller than 0.1 incurs more convergence time while that of larger than 0.2 causes more unnecessary transitions, and both resulted in less throughput. In our simulation, possible bandwidths are 20, 40 and 80 MHz and static access is used as they are mandatory. Since we focus on the effect of ARF only, we do not use RTS/CTS here; see [11] for the results on RTS/CTS.

Fig. 14 illustratesa chain of six transmitter-receiver pairs, demonstrating the effect of PoBA on performance, where APs are transmitters and handsets are receivers. Depending on the distances between neighbors and channel configurations, some AP-handset pairs suffer the HC problem. The distance and initial channel configurations are so set that AP 2 and 6 suffer the HC problem due to AP 1 and 5.

Table 5 shows the simulation results for this topology. In both closed and open loop systems, PoBA improves the throughput of AP 2 and 6. In closed systems, the algorithm improves channel utilization and decreases packet error rates. In open loop systems, error rates are already low even without PoBA because ARF adapts to the MCS level to combat bad channel conditions. So, the channel utilization is high initially. Even in such a case, PoBA enables interferee APs to raise their MCS levels by avoiding the HC collision, improving throughput.

Random topologies with a fixed number of links are generated within a 100 m $\times$ 100 m grid. Each simulation is run for 5 sec, which is sufficient for the algorithm to converge to a sub-optimal point if it exists, and each topology with the same number of links is randomly generated 100 times. The results of the simulation runs are averaged. As for the convergence, the simulation results show that the rough convergence of a belief is achievable in less than 10 action choices.[5] But detailed treatment of convergence is far more

---

4. The channel utilization is the bandwidth-time product used for successful packet transmissions over the entire available bandwidth-time resource.

5. There are 12 action choices and two trials for each action is needed on average (50 percent of hidden channel collision) to find out whether an interferee exists. In our setting, not every device has 12 interferees. So, it takes less than the maximum. This is because using larger bandwidth is beneficial and it reduces the search space.

(a) Packet error rate

(b) Throughput
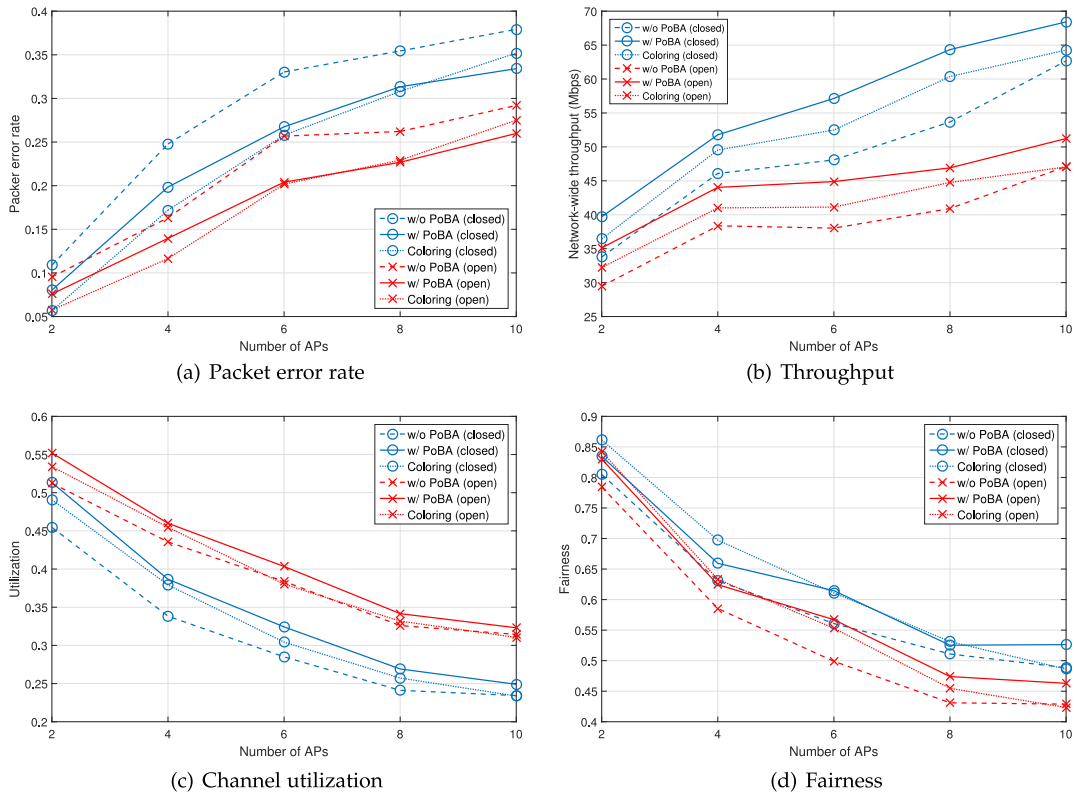

(c) Channel utilization

(d) Fairness

Fig. 15. Simulation results for random topologies.

complicated as discussed in [33], and is worth a separate paper. So, we leave it as our future work.

In Fig. 15, the node density of the network increases with the number of links in the grid. Since the size of the grid is 100 m × 100 m, 10 links crowds the topology. When the number of links is 10, the packet error rates without PoBA are 38 and 30 percent in the closed and open loop systems, respectively, as shown in Fig. 15a. The error rates are decreased by 5 percentage points for both, when PoBA is applied. These results lead to the increase of throughput per link as shown in Fig. 15b. PoBA is shown to achieve 10Mbps more throughput, 10 to 30 percent performance improvements, in both the cases.

Note that the packet error rate when the *coloring*, i.e., centralized channel assignment in [11], is applied shows a similar tendency like PoBA. However, PoBA achieves more throughput than the coloring algorithm as in Fig. 15b. The reason for this is that our PoBA is enabled to try all available bandwidth-channel configurations in real-time while the coloring algorithm fixes the configuration once assigned, thus a link with disadvantageous configuration will suffer from the starvation problem.

The ARF algorithm achieves lower packet error rate than the closed loop systems while sacrificing throughput performance as shown in the figures. This is because, like the toy example, ARF lowers MCS level to combat against the bad channel condition and HC collision, and the lowered MCS level leads to decreased throughput.

By avoiding unnecessary collisions, PoBA also increases channel utilization as shown in Fig. 15c. The performance of the coloring algorithm lies between those of with and without PoBA. This is because PoBA has all degrees of freedom in choosing a configuration in real time. Fig. 15d also shows that PoBA increases Jain's fairness index in throughput by

around 0.05 points. As the number of links increases, fairness generally decreases because some of the links can suffer from lower throughput due to regional crowdedness.

Fig. 16 shows the effects of PoBA when the grid becomes further crowded. The results for the coloring are excluded in the graph, because running the coloring for more than 10 links needs untractable computational time. As observed in the figures, PoBA effectively reduces the error rate by around 7 percent, resulting in an increment of 5 to 10 Mbps throughput steadily.

7   RELATED WORK

Another possible option to detect the HC collision in wireless networks is to exploit Multiple Input Multiple Output (MIMO) capabilities. In MIMO systems, some of antennas can transmit data while the others can be used to detect the HC collision. However, in most 802.11 cases, MIMO is used for transmitting multiple streams simultaneously to exploit diversity or multiplexing gain. Of current MIMO research is to enhance throughput performance in networks with downlink/uplink Multiple User MIMO (MU-MIMO). Mode selection per antenna in MIMO is an open research topic and not within the scope of this paper.

Likewise, a full-duplexing system [25], which enables an antenna to transmit and receive data simultaneously, can be used to detect the HC collision. Despite its potential usefulness, full-duplexing requires modification to the hardware of network interface cards. So, current off-the-shelf devices with ratified standards, such as 802.11n and 802.11ac, cannot make use of it.

Unlike MIMO and full-duplexing, post-CCA can be easily implemented by modifying firmware without any
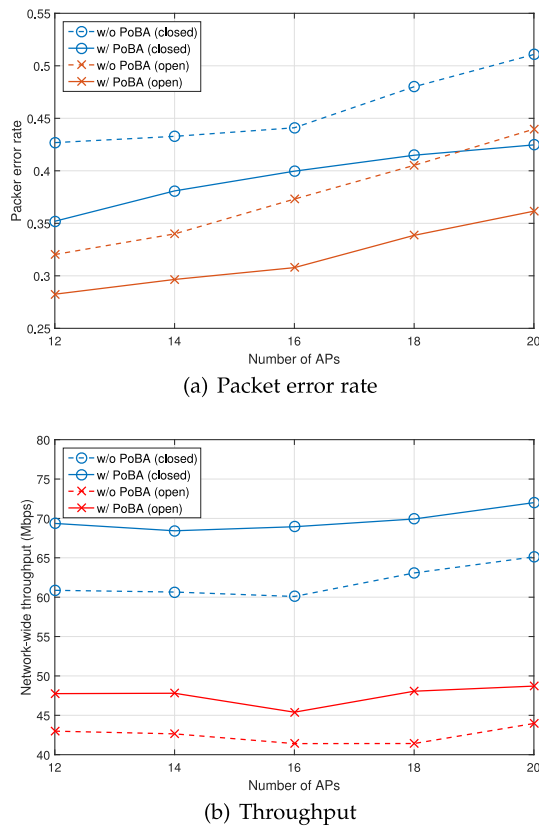
(a) Packet error rate

(b) Throughput

Fig. 16. Simulation results for random topologies with up to 20 links.

hardware modification. So, it can be applied to off-the-shelf WiFi devices by firmware upgrade. It is usually easy to modify the firmware if the firmware for commercialized Wi-Fi chipsets becomes open source.[6]

As stated earlier, the HC problem itself has been articulated and analyzed in [11]. Their approach to the problem was to use channel assignment at an access point controller (APC). All APs in a network are connected to the APC, which gathers all the APs' interfering information to make channel-assignment decisions. That is, their approach works in a centralized way and can only be applied to an enterprise network where channel configurations of APs are managed by a single APC. In contrast to this, the post-CCA and PoBA take a distributed approach to the problem, and can thus be applied to general Wi-Fi networks.

Researchers have recently studied the feasibility of dynamically changing bandwidth without modifying hardware, i.e., by only manipulating digital signal processing stages [14], [15], [16]. They claim that agile expansion or reduction of bandwidth according to the medium condition enhances transmission efficiency. We are able to use their methods of controlling bandwidth by adding an additional signal processing step, such as interpolation or subcarrier nulling at the digital baseband processing stage.

There has been a study addressing the subset of our hidden channel problem [27]. It considered the traditional problem of distinguishing the case for the second event in

Table 2, i.e., idle post-CCA without ACK. They assumed that a received packet as a whole can be delivered as a feedback to an original transmitter. Then, they determine the cause for unsuccessful transmission by comparing the transmitted and received packets.

Also, the authors of [28] proposed to selectively adopt RTS/CTS for determination of the cause of collisions, and modify the operation profile of Auto Rate Fallback according to the collision result. The granularity of CARA is finer than that of ours. Our approach changes the bandwidth-channel configuration (more macroscopic adaptation) and then apply rate adaptation.

Many researchers tackled the channel assignment problem in 802.11 networks [30], [31], [32]. Most of them target to improve network performance such as channel utilization and throughput in 802.11a/b/g networks, where multi-channels partially overlap. To the best of our knowledge, [11] is the first that analyzes the hidden channel problem, and our work extends the solution to more common cases.

8 CONCLUSION

In this paper, we presented the *hidden channel* problem that arises from use of heterogeneous bandwidths in emerging gigabit LANs. This problem reveals that the conventional CSMA/CA fails to achieve good performance in some network scenarios. We first illustrated the problem with an 802.11ac network as a reference system. We then performed simple experiments to show that the problem is real. Following that, the severeness of the HC problem and the effects of bandwidth and secondary sensitivity on network performance are shown with probabilistic analysis.

We proposed the *post-CCA* operation—i.e., another channel assessing stage after finishing a packet transmission—to alleviate the problem. The post-CCA helps mimic the CSMA/CD mechanism in the wired Ethernet to enhance the channel assess capability. The results from the post-CCA operation are used to dynamically adapt the bandwidth-channel configuration of each system in a distributed manner. For the adaptation, we designed *PoBA* that avoids the HC problem in general network topologies. PoBA improves network throughput, channel utilization and fairness performance, and decreases packet error rates.

REFERENCES

[1] WARP Project. [Online]. Available: http://www.warpproject.org
[2] National Instrument. [Online]. Available: http://www.ni.com/sdr/usrp
[3] GnuRadio. [Online]. Available: http://gnuradio.org
[4] Maxim intergrated, MAX2828/MAX2829 Single-/Dual-band 802.11a/b/g world-band tranceiver ICs. [Online]. Available: http://datasheets.maximintegrated.com/en/ds/MAX2828-MAX2829.pdf
[5] Qualcomm Inc. "The 1000x data challenge," Oct. 2013. [Online]. Available: http://www.qualcomm.com/solutions/wireless-networks/technologies/1000x-data

6. Currently, 802.11ac supporting chipsets are Qualcomm Atheros with ath10k driver and Intel WiFi chipsets with iwlwifi drivers. Since the firmware for those chipsets are not publicly open yet, we were unable to test post-CCA with them.

[6] Nokia, "Nokia LTE for unlicensed spectrum," Nokia Networks, White paper, 2014.

[7] Ericson, "LTE licensed assisted access," 2015. [Online]. Available: http://www.ericsson.com/res/thecompany/docs/press/media_kits/ericsson-license-assisted-access-laa-january-2015.pdf

[8] *HEW SG March 2014 Closing Report*, IEEE SG report, [Online]. Available: http://www.ieee802.org/11/Reports/hew_update.htm

[9] *Enhancements for Very High Throughput Operation in Bands Below 6 GHz*, IEEE Standard Amendment 802.11ac, 2011.

[10] *Enhancement for Higher Throughput*, IEEE Standard Amendment 802.11n, 2009.

[11] S. Jang and S. Bahk, "A channel allocation algorithm for reducing the channel sensing/reserving asymmetry in 802.11ac metworks," *IEEE Trans. Mobile Comput.*, vol. 14, no. 1, pp. 458–472, Mar. 2015.

[12] L. Deek, E. Garcia-Villegas , E. Belding, S.-J. Lee, and K. Almeroth, "Intelligent channel bonding in 802.11n WLANs," *IEEE Trans. Mobile Comput.*, vol. 13, no. 6, pp. 1242–1255, Jun. 2014.

[13] E. Chai, K. G. Shin, J. Lee, S.-J. Lee, and R. H. Etkin, "Fast spectrum shaping for next-generation wireless networks," *IEEE Trans. Mobile Comput.*, vol. 13, no. 1, pp. 20–34, Jan. 2014.

[14] S. Yun, D. Kim, and L. Qiu, "Fine-grained spectrum adaptation in WiFi networks," in *Proc. ACM 19th Annu. Int. Conf. Mobile Comput. Netw.*, 2013, pp. 327–338.

[15] K. Chintalapudi, B. Radunovic, V. Balan, and M. Buettner, "WiFi-NC: WiFi over narrow channels," in *Proc. ACM 9th USENIX Conf. Netw. Syst. Des. Implementation*, 2012, pp. 4–4.

[16] X. Zhang and K. G. Shin, "Adaptive subcarrier nulling: Enabling partial spectrum sharing in wireless LANs," in *Proc. IEEE Int. Conf. Netw. Protocols*, 2011, pp. 311–320.

[17] M. X. Gong, B. Hart, L. Xia, and R. Want, "Channel bounding and MAC protection mechanisms for 802.11ac," in *Proc. IEEE Global Telecommun. Conf.*, 2011, pp. 1–5.

[18] M. Park, "IEEE 802.11ac: Dynamic bandwidth channel access," in *Proc. IEEE Int. Conf. Commun.*, 2011, pp. 1–5.

[19] E. Perahia and M. X. Gong, "Gigabit wireless LANs: An overview of IEEE 802.11ac and 802.11ad," *ACM SIGMOBILE Mobile Comput. Commun. Rev.*, vol. 15, pp. 23–33, 2011.

[20] D. Qiao, S. Choi, and K. G. Shin, "Goodput analysis and link adaptation for IEEE 802.11a wireless LANs," *IEEE Trans. Mobile Comput.*, vol. 1, no. 4, pp. 278–202, Oct. 2002.

[21] D.-J. Deng, K.-C. Chen, and R.-S. Cheng, "IEEE 802.11ax: Next generation wireless local area networks," in *Proc. IEEE 10th Int. Conf. Heterogeneous Netw. Quality Rel. Secur. Robustness*, 2014, pp. 77–82.

[22] T. A. Levanen, J. Pirskanen, T. Koskela, J. Talvitie, and M. Valkama, "Radio interface evolution towards 5G and enhanced local area communications," *IEEE Access*, vol. 2, pp. 1005–1029, Sep. 2014.

[23] A. Al-Dulaimi , S. Al-Rubaye, Q. Ni, and E. Sousa, "5G communication race: Pursuit of more capacity triggers LTE in unlicensed band," *IEEE Veh. Technol. Mag.*, vol. 10, no. 1, pp. 43–51, Mar. 2015.

[24] D. Halperin, W. Hu, A. Sheth, and D. Wetherall, "Predictable 802.11 packet delivery from wireless channel measurements," in *Proc. ACM SIGCOMM Conf.*, 2010, pp. 159–170.

[25] D. Bharadia and S. Katti, "Full duplex MIMO radios," in *Proc. 11th UNENIX Conf. Netw. Syst. Des. Implementation*, 2014, pp. 359–372.

[26] L. P. Kaelbling, M. L. Littman, and A. R. Cassandra, "Planning and acting in partially observable stochastic domains," *Artif. Intell.*, vol. 101, no. 1/2, pp. 99–134, 1998.

[27] S. Rayanchu, A. Mishra, D. Agrawal, S. Sharad, and S. Banerjee, "Diagnosing wireless packet losses in 802.11: Separating collision from weak signal," in *Proc. 27th IEEE Conf. Comput. Commun.*, 2008, pp. 735–743.

[28] J. Kim, S. Kim, S. Choi, and D. Qiao, "CARA: Collisin-aware rate adaptation for IEEE 802.11 WLANs," in *Proc. 25th IEEE Int. Conf. Comput. Commun.*, 2006, pp. 1–11.

[29] H.-H. Choi, H. Lee, S. Kim, and I.-H. Lee, "Throughput analysis and optimization of distributed collision detection protocols in dense wireless local area networks," *J. Commun. Netw.*, vol. 18, no. 3, pp. 502–512, Jun. 2016.

[30] K. K. Leung and B.-J. Kim, "Frequency assignment for IEEE 802.11 wireless networks," in *Proc. IEEE 58th Veh. Technol. Conf.*, 2003, pp. 1422–1426.

[31] M. Yu, H. Luo, and K. K. Leung, "A dynamic radio resource management technique for multiple APs in WLANs," *IEEE Trans. Wireless Commun.*, vol. 5, no. 7, pp. 1910–1919, Jul. 2006.

[32] A. Mishra, S. Banerjee, and W. Arbaugh, "Weighted coloring based channel assignment for WLANs," *ACM SIGMOBILE Mobile Comput. Commun. Rev.*, vol. 9, pp. 19–31, 2005.

[33] C. J. C. H. Watkins, "Learning from delayed rewards," PhD Dissertation, Univ. Cambridge, Cambridge, U.K., 1989.

Seowoo Jang received BS and MS degrees from the School of Electrical Engineering & Computer Science, Seoul National University, in 2007 and 2009, respectively, and the PhD degree from Seoul National University, in 2015. He was also a visiting scholar with the University of Michigan, Ann Arbor, in 2014-2015. He is currently a senior software engineer at Samsung Electronics. His research interests include wireless MAC protocol and network optimization in cellular LTE, next-generation WLAN systems, and IoT systems. His research area also include intra and inter vehicular communication systems and automotive data processing with deep learning. He is a student member of the IEEE.

Kang G. Shin is the Kevin & Nancy O'Connor professor of computer science in the Department of Electrical Engineering and Computer Science, The University of Michigan, Ann Arbor. His current research focuses on computing systems and networks as well as on embedded real-time and cyber-physical systems, all with emphasis on timeliness, security, and dependability. He has supervised the completion of 78 PhDs, and authored/coauthored more than 900 technical articles (about 320 of these are in archival journals), one a textbook and more than 30 patents or invention disclosures, and received numerous best paper awards, including the Best Paper Awards from the 2011 ACM International Conference on Mobile Computing and Networking (MobiCom2011), the 2010 and 2000 USENIX Annual Technical Conferences, as well as the 2003 IEEE Communications Society William R. Bennett Prize Paper Award and the 1987 Outstanding IEEE Transactions of Automatic Control Paper Award. He has also received several institutional awards, including the Research Excellence Award in 1989, Outstanding Achievement Award in 1999, Distinguished Faculty Achievement Award in 2001, and Stephen Attwood Award in 2004 from The University of Michigan (the highest honor bestowed to Michigan Engineering faculty), a Distinguished Alumni Award of the College of Engineering, Seoul National University in 2002; 2003 IEEE RTC Technical Achievement Award, and 2006 Ho-Am Prize in Engineering (the highest honor bestowed to Korean-origin engineers). He has chaired several major conferences, including 2009 ACM MobiCom, 2008 IEEE SECON, 2005 ACM/USENIX MobiSys, 2000 IEEE RTAS, and 1987 IEEE RTSS. He has also served or is serving on numerous government committees, such as the US National Science Foundation Cyber-Physical Systems Executive Committee and the Korean Government R&D Strategy Advisory Committee. He has also co-founded a couple of startups. He is the life fellow of the IEEE and a fellow of the the ACM.

Saewoong Bahk (M'94-SM'06) received BS and MS degrees in electrical engineering from Seoul National University, in 1984 and 1986, respectively, and the PhD degree from the University of Pennsylvania, in 1991. From 1991 through 1994, he was with AT&T Bell Laboratories as a member of technical staff where he worked for network management. In 1994, he joined the School of Electrical Engineering, Seoul National University and currently serves as a professor. He has been serving as a TPC member for various conferences including ICC, GLOBECOM, INFOCOM, PIMRC, WCNC, etc. He was TPC chair for the IEEE Vehicular Technology Conference (VTC)-2014 Spring. He was awarded for excellent teaching and excellent performance from the Engineering College at Seoul National University in 2010 and 2013, respectively. He is co-editor-in-chief of the *Journal of Communications and Networks*, and was on the editorial boards of the *IEEE Transaction on Wireless Communications*, and the *Computer Networks Journal*. His areas of interests include performance analysis of communication networks and network security. He is a senior member of the EEE and a member of Who's Who Professional in Science and Engineering.